PHYSICAL REVIEW B **85**, 113302 (2012)

Kinetics of *a*-Si:H bulk defect and *a*-Si:H/*c*-Si interface-state reduction

Stefaan De Wolf,[1,*] Christophe Ballif,[1] and Michio Kondo[2]
[1]*École Polytechnique Fédérale de Lausanne (EPFL), Institute of Microengineering (IMT), Photovoltaics and Thin Film Electronics Laboratory, Rue A.-L. Breguet 2, CH-2000 Neuchâtel, Switzerland*
[2]*National Institute of Advanced Industrial Science and Technology (AIST), Central 2, 1-1-1 Umezono, Tsukuba, Ibaraki 305-8568, Japan*
(Received 20 July 2011; revised manuscript received 21 November 2011; published 19 March 2012)

Low-temperature annealing of hydrogenated amorphous silicon (*a*-Si:H) is investigated. An identical energy barrier is found for the reduction of deep defects in the bulk of *a*-Si:H films and at the interface such layers form with crystalline Si (*c*-Si) surfaces. This finding gives direct physical evidence that the defects determining *a*-Si:H/*c*-Si interface recombination are silicon dangling bonds and that also kinetically this interface has no unique features compared to the *a*-Si:H bulk.

DOI: 10.1103/PhysRevB.85.113302 PACS number(s): 73.61.Jc, 71.55.−i, 73.20.Hb, 81.40.Ef

Hydrogenated amorphous silicon (*a*-Si:H) is a semiconductor with practical applications in a range of large-area electronic devices, including thin-film solar cells.[1] Remarkably good electronic passivation of crystalline Si (*c*-Si) surfaces can be obtained with *a*-Si:H films of only a few nanometers thin as well. This enables the fabrication of high-efficiency *a*-Si:H/*c*-Si heterojunction solar cells.[2,3] The *a*-Si:H/*c*-Si interface is of equal importance in device-grade microcrystalline Si, which is used as a red-light absorber in thin-film Si tandem solar cells.[1] This material consists of nano-sized *c*-Si grains embedded in an *a*-Si:H host matrix. Recently, it was pointed out that the *a*-Si:H/*c*-Si interface may not possess unique properties compared to the *a*-Si:H bulk.[4] An experimental proof by direct comparison between *a*-Si:H/*c*-Si interface and *a*-Si:H bulk has been lacking so far, however.

In this Brief Report, we perform this comparison kinetically and find that the *a*-Si:H bulk and *a*-Si:H/*c*-Si interface essentially face the same energy barrier for deep-defect reduction. This physically validates the assumption that the defects determining *a*-Si:H/*c*-Si interface recombination are silicon dangling bonds (DB). This barrier does not depend on any film property. This contrasts with the optimal *c*-Si surface passivation obtainable by *a*-Si:H, which strongly depends on the precise Si-H bonding configuration of the film.

For the experiments, intrinsic *a*-Si:H films were deposited using a plasma-enhanced chemical vapor deposition reactor operated at radio frequency (rf, 13.56 MHz) power. The deposition temperature, T_{depo}, was varied between 70 and 230 °C. For substrates, either mirror-polished boron-doped float zone FZ-Si(100) wafers (300 μm, ∼3.0 Ω cm) or quartz samples were used. The deposition rate was in all cases ∼1 Å s^{-1}. Further deposition and sample cleaning details are given elsewhere.[5] For all conditions, identical films of ∼50 nm thick were deposited on both wafer surfaces to evaluate the interface-passivation quality. On quartz, ∼1.2-μm-thick films were deposited to allow for electron spin resonance (ESR) measurements, probing paramagnetic defect densities. Following deposition, the samples underwent a stepped low-temperature annealing cycle in vacuum (30-min steps, with the annealing temperature T_{ann} ranging from 120 to 260 °C in 20 °C increments). In between these steps, the value for the effective carrier lifetime τ_{eff} of the wafers was measured by the quasi-steady-state photoconductance (QSSPC) technique.[6] Since high-grade *c*-Si substrates were used, the measured τ_{eff} value is a direct indicator for the passivation quality of the *a*-Si:H films. Similarly, the spin density of the films on quartz was measured in between annealing steps. For this, four samples of about 0.5 × 1.0 cm^2 featuring identical films were stacked perpendicular to the magnetic field in a Bruker EMX EPR spectrometer. The field sweep width was 100 G, centered around 3415 G. The microwave power was 1.008 mW, whereas the frequency varied between 9.585 and 9.603 GHz. The absolute spin density was obtained by comparison to a calibrated sample. Both QSSPC and ESR were measured at room temperature. Finally, to gain insight in the Si-H bonding environment in thin *a*-Si:H films, thermal desorption spectroscopy (TDS) measurements were performed. The heating rate was 20 K min^{-1}.

The influence of T_{depo} on the *a*-Si:H/*c*-Si interface-passivation quality is given in Fig. 1(a). Two distinct regimes are present: For sufficiently low T_{depo}, the stepped annealing cycle (i.e. after all annealing steps, including the final 260 °C step) yields improved interface passivation. At higher T_{depo}, such annealing leads to electronic losses, however. This transition principally occurs when (low-quality) epitaxial growth of Si was initiated at the interface during deposition,[5] which is also detrimental to *a*-Si:H/*c*-Si heterojunction solar cell performance.[7] The samples deposited at $T_{\mathrm{depo}} > 200$ °C were confirmed to feature fully epitaxially grown interfaces.[5] Figure 1(b) shows the optical bandgap $E_{\mathrm{G}}^{\mathrm{opt}}$ (determined from spectroscopic ellipsometry, using the Tauc–Lorentz model as discussed by Ferlauto *et al.*)[8] of those films that were epitaxy free, measured after the final 260 °C anneal. Here, $E_{\mathrm{G}}^{\mathrm{opt}}$ decreases gradually with higher T_{depo}, which often points to a gradually lower bonded hydrogen content of the films.[9]

For bulk *a*-Si:H, a link between hydrogen content and electronic defect density is known to exist. More precisely, the lowest electron-spin density is obtained for those films with a dominant lower Si-H bond stretching frequency,[10] corresponding to nano-void lean material. To verify this relation also for *a*-Si:H/*c*-Si interfaces, the TDS measurements of Fig. 1(c) give more detailed information of the hydrogen content of the passivation films, compared to spectroscopic ellipsometry. For intrinsic *a*-Si:H material, TDS measurements typically reveal two H_2-effusion peaks, which can be fairly well deconvoluted by Gaussians (for films with atomically

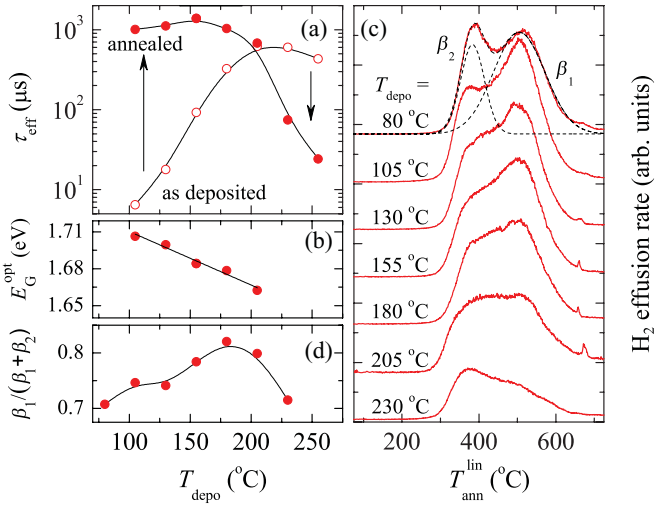

FIG. 1. (Color online) (a) Influence of T_{depo} on a-Si:H/c-Si interface-passivation quality. Results before (open symbols) and after (closed symbols) stepped low-temperature annealing are shown. Evaluation at $\Delta n = 1.0 \times 10^{15}$ cm^{-3}. (b) Optical bandgap of the films. (c) Thermal desorption spectroscopy data for the films shown in (a). For clarity, the data have been offset vertically. (d) $\beta_1/(\beta_1 + \beta_2)$ ratio, taken from the TDS data. Solid lines in (a), (b), and (d) are guides for the eye.

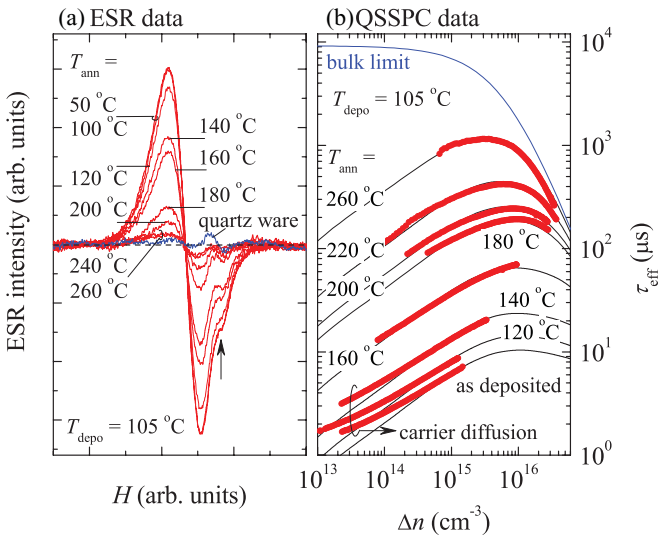

FIG. 2. (Color online) (a) Electron spin resonance data for a ∼1.2-μm-thick a-Si:H film deposited at 105 °C on quartz. For reference, the signal of the quartz ware is given, too. (b) τ_{eff} vs Δn data, for ∼50-nm-thick a-Si:H films deposited at 105 °C, deposited on a p-type Si(100) wafer. Measurements (symbols) made by QSSPC method. Solid lines are calculated fits. The uppermost curve shows the bulk-limited value for τ_{eff}. Results before and after step-wise annealing are shown.

sharp interfaces, as shown in Fig. 1(c) for the lowest T_{depo} data). A dominant lower-temperature peak, β_2, points to the presence of (interconnected) hydrogen-terminated internal voids and surfaces in the film.[11] The higher-temperature peak β_1 is rather a signature for dense material rich in monohydrides. Figure 1(d) gives the $\beta_1/(\beta_1 + \beta_2)$ peak-intensity ratio, indicative for the film density. Figure 1 shows that the best (annealed) passivation is obtained at deposition temperatures slightly lower than for the densest layers. We attribute this difference to the presence of mixed-phase material at the interface, for the densest films. Similar to the a-Si:H bulk, we conclude that, for a-Si:H/c-Si structures, the best electronic properties are obtained for the densest films, under the necessary condition that their interface is completely epitaxy free, however.

We remark here that improved a-Si:H/c-Si interface passivation by annealing recently was explained by a model where (two) Si DBs may (reversibly) convert into a strained Si-Si bond.[4] In this model, first proposed by Stutzmann for the a-Si:H bulk,[12,13] the distribution of strained Si-Si bonds (often expressed by a disorder parameter E_0) dictates the DB density, N_{DB}. The value of E_0 is intrinsically linked to film growth[14] (and thus deposition conditions), with the lowest values for dense films, lean in nano-voids.[15] As low values of E_0 enable low values for N_{DB},[13] this weak-bond model may explain how dense a-Si:H films are usually found to be electronically superior, either from bulk or surface-passivation perspective.

We now turn to the kinetics that drive the defect reduction in the atomically sharp a-Si:H/c-Si structures. For reference, first, we present defect-annealing data for the bulk of a-Si:H films. Figure 2(a) shows ESR data for a ∼1.2-μm film deposited at very low temperature (105 °C) on quartz. Electron spin resonance measurements only probe singly occupied states. The decrease in ESR signal following annealing points to a reduction of neutral-spin density in the film, confirming the benign effect of (low-temperature) annealing on the electronic properties of the a-Si:H bulk.[16] The depression in the data (see arrow) is likely caused by the quartz ware in the sample cavity (such as due to the SiO_2 E' defect).[17]

Figure 3(a) shows neutral-spin densities N_S^0 for films deposited at indicated temperatures and extracted from raw

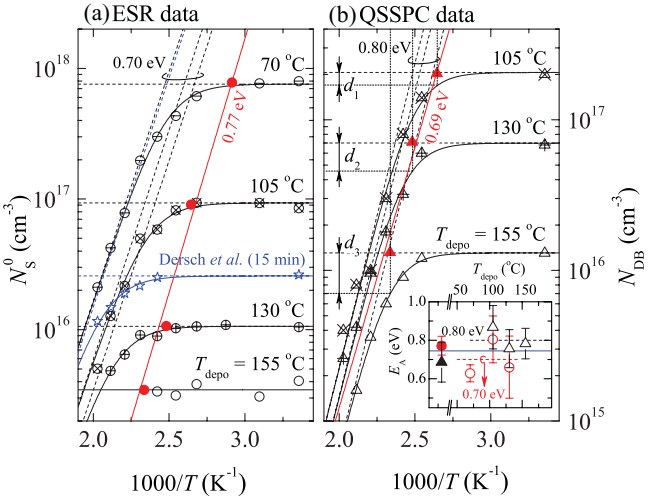

FIG. 3. (Color online) (a) Annealing dependence of ESR spin densities for ∼1.2-μm-thick a-Si:H films on quartz substrates. (b) Annealing dependence of calculated interface-defect densities for a-Si:H/c-Si interfaces. Film thickness is ∼50 nm. In both panels, for the open (closed) symbols, the abscissa represents the inverse of the annealing (deposition) temperature. Solid lines are fits to an energy barrier, including baseline correction. Inset shows the fitted E_A values. Discs: ESR data; triangles: QSSPC data. Dashed lines show multifit values for either case.

ESR data, similar to those given in Fig. 2(a). In Fig. 3(a), we superpose two data sets. The first set shows the effect of T_{depo} on N_S^0 and is marked with closed symbols. Here, the abscissa represents the inverse of T_{depo}, and an activation energy E_A of ∼0.77 eV is found. The second set shows the effect of annealing on N_S^0 and is marked with open symbols. Here, the abscissa represents the inverse of T_{ann}. The annealing steps were 30 min long, the actual depositions took as long as 3 h. In our experimental setup, the spin-density detection limit was about 3.0×10^{15} cm^{-3}. After baseline correction, the annealing-induced spin-density decay follows an Arrhenius law as well. This is shown by the solid fitting curves given by $N_S^0 = (A + B\exp(-{}^{E_A}/_{kT_{ann}}))^{-1}$, where A and B are fitting constants and k the Boltzmann factor. Interestingly, when cofitting these data, a common value for $E_A = 0.70$ eV is found, close to the barrier found earlier. We remark at this point that Fig. 3(a) includes annealing-induced decay of light-induced spin densities, taken from Dersch *et al*. (using annealing steps of 15 min).[18] Again, satisfying fits to the same barrier can be obtained, underlining that the same defect is involved here also.

Regarding a-Si:H/c-Si interface states, Fig. 2(b) gives injection-level dependent carrier-lifetime data of a sample with 50-nm-thin a-Si:H films, also deposited at a very low temperature. Again, data at different values for T_{ann} are shown. Figure 3(b) gives DB densities N_{DB} for a-Si:H/c-Si structures deposited at indicated temperatures, extracted from such measurements. To do so, the lifetime data were fitted to an a-Si:H/c-Si interface-recombination model (see solid lines) which yields two major model parameters: The surface DB density N_{DB}^S and the fixed-charge density Q_f, comprising all contributions to the surface potential.[19–21] Electronically, DBs are characterized by their electron and hole capture cross sections in the neutral (σ_n^0 and σ_p^0) and charged states ($\sigma_n{}^+$ and $\sigma_p{}^-$), respectively. The following ratios (similar to the a-Si:H bulk) were found for the interface DB capture cross sections:[20] $\sigma_p^0/\sigma_n^0 = 20$ and $\sigma_n{}^+/\sigma_n^0 = \sigma_p{}^-/\sigma_p^0 = 500$. Satisfying fits to the shown datasets can then be obtained by only adjusting N_{DB}^S (Q_f is kept constant at 7.5×10^{10} cm^{-2}).[22] This shows that annealing changes the surface-state density but not the surface band bending, within fitting error; pointing to chemical rather than field-effect passivation at the a-Si:H/c-Si interface.[4,19,21] Finally, we convert N_{DB}^S in a bulk equivalent N_{DB}, supposedly probed by the electron wave function at the c-Si surface.[4,21] For this, all QSSPC extracted N_{DB}^S data were divided by an *ad-hoc* probing depth D, so that the as-deposited N_{DB} value equaled the arbitrarily but reasonably chosen value of 2.0×10^{17} cm^{-3}, for the films deposited at 105 °C. With $\sigma_p^0 = 5 \times 10^{-16}$ cm^2, we obtain $D = 10$ nm, which is a realistic value.

In Fig. 3(b), we again superpose two datasets. The first set shows the effect of the value for T_{depo} on N_{DB} and is marked with closed symbols. Here, the abscissa represents the inverse of T_{depo}, and we find a ∼0.69 eV barrier, which is close to the one found for bulk a-Si:H defects. The second set shows the effect of annealing on N_{DB} and is marked with open symbols. Here, the abscissa represents the inverse of T_{ann}. We can again fit all data to the earlier given relation. Here $E_A = \sim 0.80$ eV, independent from the earlier chosen value D. The inset shows the individual estimates for E_A, including the averages for both structures. Considering this narrow range, both the spin density in the a-Si:H bulk and the a-Si:H/c-Si interface-defect density arguably face a common energy barrier of ∼0.74 eV, within experimental error (see solid line in inset).

The common activation energy for defect reduction upon annealing in a-Si:H bulk and at the a-Si:H/c-Si interface points to the removal of the same type of defect in both cases. Regarding its nature, the dominant defect in the a-Si:H bulk features an ESR signal at a g value of 2.0055 [which is the defect probed in Figs. 2(a) and 3(a)]. Inspired by a similar resonance occurring at clean cleaved Si surfaces,[23] this defect is usually interpreted as a so-called Si DB, linked to a threefold coordinated Si atom.[24] The common energy barriers found here give direct experimental evidence that the defect probed by carrier-lifetime measurements at the a-Si:H/c-Si interface is an Si DB as well. Based on this, we confirm experimentally that the a-Si:H/c-Si interface does not possess unique properties compared to the a-Si:H bulk.

Finally, we remark that for the a-Si:H/c-Si structures, defect reduction starts already at $T_{\text{ann}} < T_{\text{depo}}$ [as seen in Fig. 3(b), e.g. by the deviations $d_{i=1-3}$ taken at $T_{\text{ann}} = T_{\text{depo}}$]. This most likely is due to the short deposition times for these samples. For the much thicker ESR samples of Fig. 3(a), this phenomenon is not observable, confirming that, underneath the film-growth surface, *in-situ* defect annealing may occur.[25,26]

In summary, a universal energy barrier for defect reduction is found. Its value is the same for a-Si:H bulk defects and a-Si:H/c-Si interface states, independent of film properties. This gives direct experimental proof that Si dangling bonds are the source of recombination in both systems. Conversely, deposition conditions affect the silicon-to-hydrogen configuration of a-Si:H which, in turn, affect the film disorder. Such disorder sets a limitation to the minimal achievable deep-defect density. The universal energy barrier physically validates carrier-lifetime measurements to extract (relative) dangling-bond densities.

SDW thanks H. F. W. Dekkers, F. J. Haug, and T. F. Schulze for useful discussions. This work was supported by NEDO, Japan, by the European Community's FP7 Programme under the 20plμs Project (Grant Agreement No. 256695), and by Axpo Naturstrom Fonds, Switzerland.

*Corresponding author: stefaan.dewolf@epfl.ch

[1] A. Shah, P. Torres, R. Tscharner, N. Wyrsch, and H. Keppner, Science **285**, 692 (1999).

[2] T. Mishima, M. Taguchi, H. Sakata, and E. Maruyama, Sol. Energy Mater. Sol Cells **95**, 18 (2011).

[3] S. De Wolf, A. Descoeudres, Z. C. Holman, and C. Ballif, Green **2** doi: 10.1515/green-2011-0039.

[4] T. F. Schulze, H. N. Beushausen, C. Leendertz, A. Dobrich, B. Rech and L. Korte, Appl. Phys. Lett. **96**, 252102 (2010).

[5] S. De Wolf and M. Kondo, Appl. Phys. Lett. **90**, 042111 (2007).

[6]R. A. Sinton and A. Cuevas, Appl. Phys. Lett. **69**, 2510 (1996).
[7]T. H. Wang, E. Iwaniczko, M. R. Page, D. H. Levi, Y. Yan, H. M. Branz, and Q. Wang, Thin Solid Films **501**, 284 (2006).
[8]A. S. Ferlauto, G. M. Ferreira, J. M. Pearce, C. R. Wronski, R. W. Collins, X. Deng, and G. Ganguly, J. Appl. Phys. **92**, 2424 (2002).
[9]A. Matsuda, M. Matsumura, S. Yamasaki, H. Yamamoto, T. Imura, H. Okushi, S. IIzima, and K. Tanaka, Jpn. J. Appl. Phys. **20**, L183 (1981).
[10]J. C. Knights, G. Lucovsky, and R. J. Nemanich, J. Non-Cryst. Solids **32**, 393 (1979).
[11]W. Beyer and H. Wagner, J. Non-Cryst. Solids **59**, 161 (1983).
[12]M. Stutzmann, Philos. Mag. B **56**, 63 (1987).
[13]M. Stutzmann, Philos. Mag. B **60**, 531 (1989).
[14]J. Robertson, J. Appl. Phys. **87**, 2608 (2000).
[15]A. H. Mahan, P. Menna, and R. Tsu, Appl. Phys. Lett. **51**, 1167 (1987).
[16]D. K. Biegelsen, R. A. Street, C. C. Tsai, and J. C. Knights, Phys. Rev. B **20**, 4839 (1979).
[17]R. A. Weeks, J. Appl. Phys. **27**, 1376 (1956).
[18]H. Dersch, J. Stuke, and J. Beichler, Appl. Phys. Lett. **38**, 456 (1981).
[19]S. De Wolf, S. Olibet, and C. Ballif, Appl. Phys. Lett. **93**, 032101 (2008).
[20]S. Olibet, E. Vallat-Sauvain, and C. Ballif, Phys. Rev. B **76**, 035326 (2007).
[21]S. De Wolf, B. Demaurex, A. Descoeudres, and C. Ballif, Phys. Rev. B **83**, 233301 (2011).
[22]The data of the lowest quality films cannot be fitted well at low injection, likely because generated carriers in the wafer need sufficient time to diffuse to the surfaces before they can recombine. This sets a minimum to the experimental carrier lifetime.
[23]D. Haneman, Phys. Rev. **170**, 705 (1968).
[24]M. H. Brodsky and R. S. Title, Phys. Rev. Lett. **23**, 581 (1969).
[25]G. N. Parsons, C. Wang, M. J. Williams, and G. Lucovsky, Appl. Phys. Lett. **56**, 1895 (1990).
[26]H. C. Neitzert, W. Hirsch, and M. Kunst, Phys. Rev. B **47**, 4080 (1993).